NASA CONTRACTOR REPORT

NASA CR-540

BUCKLING OF CYLINDRICAL SHELL END CLOSURES BY INTERNAL PRESSURE

by G. A. Thurston and A. A. Holston, Jr.

BUCKLING OF CYLINDRICAL SHELL END CLOSURES

BY INTERNAL PRESSURE

By G. A. Thurston and A. A. Holston, Jr.

CONTENTS

BUCKLING OF CYLINDRICAL SHELL END CLOSURES

BY INTERNAL PRESSURE

By G. A. Thurston and A. A. Holston, Jr.
Martin-Marietta Corporation

SUMMARY

A theoretical study was conducted on buckling of shallow end closures of cylindrical shells under internal pressure. The most important result from the analysis is that elliptical domes can be designed that do not buckle under internal pressure although they are shallower than the $\sqrt{2}:1$ elliptical domes in common use in aerospace vehicles. This indicates that decreasing the rise of elliptical domes could result in a weight savings because of shortening the structure between tanks and stages of missiles.

Finite-deflection theory was used to compute the prebuckling stress distribution. This theory predicts that the rate of change of compressive circumferential stresses as a function of pressure decreases as the internal pressure increases. This nonlinear relationship between hoop stress and pressure results in computed bifurcation pressures for asymmetric wrinkling that are higher than buckling pressures from linear theory and predicts that some closures do not buckle under any pressure.

INTRODUCTION

Torispherical and elliptical shells are commonly used as end closures for cylindrical pressure vessels. The "square root of two to one" elliptical dome has become virtually sacrosanct for propellant tanks in certain aerospace vehicles. This ratio of cylinder radius to dome rise is derived from membrane theory by postulating that no circumferential compressive stress should appear in the dome due to internal pressure. With no compressive stresses, there can be no problem of designing for buckling due to internal pressure.

This approach would appear to be conservative for two reasons. First, the cylinder and any skirts will support the edge of the dome so that membrane theory will not apply. This support resists the inward radial displacements that must accompany compression and lowers the level of compressive stresses from that predicted from membrane theory. Second, the dome will have enough stiffness to prevent buckling if the compressive stresses are not too high.

This report contains theoretical results that provide some insight into pressure levels that can be expected to produce wrinkling in shallow domes.

The torispherical dome consists of a spherical cap joined to a toroidal segment, joined in turn to the cylindrical pressure vessel. Galletly (ref. 1) warned that membrane theory is not adequate for predicting stresses in the toroidal portion of torispherical heads and proceeded to compute stresses based on linear bending theory. He noted the possibility of elastic buckling due to the compressive hoop stresses that can be developed. Mescall (ref. 2) calculated pressures that would produce asymmetric buckling modes in torispherical shells. He used linear bending theory to compute the prebuckling stress state based on an asymptotic solution by Clark (ref. 3) and a Rayleigh-Ritz procedure to compute bifurcation pressures from a Donnell-type buckling theory.

The present analysis goes a step further by computing the axisymmetric stresses from nonlinear finite-deflection theory and the buckling pressures from an improved theory. The results are compared with Mescall's data and with experimental buckling pressures reported by Adachi and Benicek (ref. 4). The compressive circumferential stresses predicted by the nonlinear theory are lower than those from linear theory, and the agreement between the computed and experimental buckling pressures is good.

The elliptical end closure has apparently not been studied as extensively as the torispherical shell. The present study indicates that elliptical domes can be shallower than $\sqrt{2}:1$ without buckling from internal pressure and that the amount of reduction in shallowness depends on the ratio of thickness to minor axis. The use of shallower closures for space vehicle propellant tanks would provide a twofold reduction in weight. First, the closure would be lighter since it would be shallower, and second, since the closure would be shallower, the distance between tanks could be reduced.

SYMBOLS

a	radius of spherical cap
C	extensional stiffness, $Eh/(1 - \nu^2)$
C_{ij}	influence coefficients
$ds = \alpha_o dx$	element of arc length of shell
h	shell thickness
H^o	axisymmetric horizontal stress resultant
k_1	curvature of meridian of undeformed shell
ℓ	rise of torispherical closure
m	minor axis of elliptical closure
M_x^o	axisymmetric meridional stress couple
n	number of circumferential waves of buckling mode
N_x^o, N_θ^o	axisymmetric stress resultants in meridional and circumferential directions, respectively
q	internal pressure
q_{cr}	critical internal pressure for asymmetrical buckling
Q_x^o	axisymmetric transverse stress resultant
R_c	cylinder radius
r_o	horizontal radius to generic point of the undeformed shell
R_t	toroidal radius
u^o	axisymmetric radial deflection

β_x^o axisymmetric rotation of shell normal

ν Poisson's ratio

φ_o angle from centerline to normal of shell

$\bar{\varphi}_o$ opening angle of spherical cap portion of tori-spherical closure

                        differentiation with respect to the independent variable x

THEORY

The differential equations for shells of revolution used in the analysis are derived in reference 5, and that derivation will not be repeated here.

The main feature of the theory is computing the prebuckled state of stress from nonlinear finite-deflection equations rather than assuming that membrane theory is adequate. At certain critical loads, bifurcation occurs with asymmetric equilibrium positions existing infinitesimally near the axisymmetric equilibrium state. The bifurcation points are determined from linearized theory.

The same approach has been used recently by several authors for special cases of shallow spherical caps (refs. 6 thru 8), cylinders under axial compression (refs. 9 and 10), and cones under external pressure (ref. 11).

The analysis in reference 5 uses Reissner's finite-deflection equations for shells of revolution under axisymmetric loads as the basis for the prebuckled stress distribution. The linearized equations for computing the critical loads are derived from the nonlinear strain-displacement relations with lines of curvature coordinates listed by Sanders (ref. 12).

Weinitschke (ref. 7) has an extensive discussion of the pertinent equations for the special case of the shallow spherical shell. The differential equations are written in operator notation, which makes it easy to see the differences between the present approach and classical solution. Reference 5 contains the equations for a general shell of revolution.

The prebuckled solution requires solving a fourth order set of nonlinear ordinary differential equations. The bifurcation points are defined by nontrivial solutions of a set of homogeneous eighth order linear partial differential equations.

In references 6 and 11, the solutions of the homogeneous equations were found by successive approximations. When this iterative procedure was applied to the case of spherical caps under point load (ref. 5), it failed to converge. Convergence problems also appeared in the present study of domes under internal pressure. The exact cause of the lack of convergence was not ascertained, but both problems were characterized by tensile stresses existing along with the compressive stresses that cause buckling.

The computer program for the numerical solution of the differential equations was rewritten to solve these problems directly by relating critical loads to the vanishing of a determinant. The change in the numerical solution involved shifting vectors from the right-hand side of a matrix equation and adding them to other vectors appearing on the left side to make a set of linear homogeneous algebraic equations approximating the homogeneous differential equations.

The additional terms are listed in the appendix. The computer program is written so that three separate shell theories can be checked by the solution, depending on terms retained in the vectors. If only the terms in the appendix that are underlined twice are added, the result is a Donnell-type theory where the expressions for changes of curvature during buckling contain only w, the component of displacement normal to the undeformed shell. If the terms in the appendix with a single underline are also added, the result will be analogous to Flugge's theory for cylinders (ref. 13) where the prebuckled stress resultants enter all three equilibrium equations. Finally, if the terms in the appendix containing β_x^o that are not underlined are added along with the rest, the complete set of terms consistent with linearizing Sanders' equations (ref. 12) are retained. The terms in β_x^o are difficult to explain on physical grounds, but they reflect the change in strain-displacement relations of the shell due to the prebuckling rotation β_x^o of the shell normal.

The critical loads are dependent on the boundary conditions assumed for the dome in the prebuckled state and during buckling. The boundary conditions for the axisymmetric prebuckled solution were varied. Some of the runs assumed that the domes were attached to a cylinder of the same material and thickness as the dome. These solutions are denoted in the results as "cylinder boundary conditions." The limiting case of a stiffer support was obtained by using "clamped" conditions with no radial deflection or edge rotation (fig. 1).

The other limiting case of flexibility was obtained by using "membrane" conditions with no edge transverse shear or moment,

$$Q_x^O = M_x^O = 0$$

In the present study, the boundary conditions for asymmetric buckling modes were restricted to clamped edges; all three components of displacement for the asymmetric solution plus the edge rotation vanish at the boundaries.

Since the prebuckled theory is nonlinear, the effect of pressure on the cylinder must be considered in computing its stiffnesses. The same is true in matching the spherical part of the torispherical dome to the toroidal knuckle. Good approximations for the effect of internal pressure on the edge stiffness of cylinders and spheres have been published by Grossman (ref. 14) and Cline (ref. 15). Cline (ref. 15) computes influence coefficients for a spherical cap from edge stresses added to the primary stress state. His equations at the edge of the spherical cap can be written

$$u^O = C_{11}\left(H^O - \frac{qa}{2}\cos\bar{\phi}_o\right) + C_{12}\,M_x^O + \frac{qa^2}{2Eh}(1 - \nu)\sin\bar{\phi}_o$$

$$\beta_x^O = C_{12}\left(H^O - \frac{qa}{2}\cos\bar{\phi}_o\right) + C_{22}\,M_x^O$$

The deformations and stress resultants must be continuous at the edge juncture of the spherical cap and the toroidal knuckle. Therefore, the above equations become two boundary conditions for the numerical solution of Reissner's equation for the toroidal

6

shell. The program accepts them by listing as input the coefficients of u^o, β_x^o, H^o, M_x^o, and the constant term from the equations written in the form

$$u^o - C_{11} H^o - C_{12} M_x^o = \frac{qa}{2} \left[\frac{a}{Eh} (1 - \nu) \sin \bar{\phi}_o - C_{11} \cos \bar{\phi}_o \right]$$

$$\beta_x^o - C_{12} H^o - C_{22} M_x^o = - \frac{qa}{2} C_{12} \cos \bar{\phi}_o$$

The influence coefficients C_{11}, C_{12}, and C_{22} are a function of the pressure q and decrease in magnitude as the shell gets stiffer with increasing pressure. The influence coefficients are computed from Cline's solution (ref. 15) in an IBM 1620 program that punches the proper input cards for the main IBM 7090 program.

A similar set of influence coefficients is computed as a function of pressure for the cylinder (ref. 14) and these appear in the other two boundary conditions for the toroidal shell.

NUMERICAL RESULTS

The numerical buckling loads obtained in this study for torispherical and elliptical closures subjected to internal pressure are summarized in tables 1 and 2. These results are also plotted in figures 2 through 10 and they will be discussed in this section.

In checking out the computer program, several runs were made on a torispherical shell discussed by Mescall (ref. 2). He used a Rayleigh-Ritz solution, which should give an upper bound to the buckling pressure, but the first computed buckling pressure was even higher than Mescall reported. The reason for the apparent discrepancy was from using different theories. Different buckling pressures from different theories are tabulated:

7

Axisymmetric theory for prebuckled stresses	Asymmetric bifurcation theory	Buckling pressure, psi
Linear	Donnell (numerical)	58
Linear	Donnell (Rayleigh-Ritz) (ref. 2)	64
Linear	Sanders (ref. 12)	53.5
Finite-deflection	Sanders (ref. 12)	67.5

The difference between linear theory and finite-deflection theory for the prebuckled stress distribution of the shell is illustrated in figure 2. The magnitude of the compressive stresses from nonlinear theory are lower for a given pressure.

The buckling pressures in the rest of the report were computed using finite-deflection theory for the prebuckled stresses and Sanders' strain-displacements relations in the asymmetric equations for bifurcation pressures. Poisson's ratio was set at $\nu = 0.3$.

The numerical results for elliptical closures are presented in table 1. The symbols used are shown in fig. 4, and the column showing the boundary conditions refers to the conditions at the juncture of the elliptical closure with the cylinder.

Similar results are presented in table 2 for torispherical closures subjected to internal pressure and the symbols used are shown in fig. 3. The column denoted by $\frac{1}{\varphi_o} \tan^{-1} \frac{\ell}{R_c}$ represents the deviation of the torisphere from a torisphere that approximates an ellipse.

A method for graphically constructing an approximate ellipse is the "four-center method." This method produces a torisphere that intersects the axes at the same points as the given ellipse. Since a torispherical closure is a three-parameter curve and an elliptical closure is a two-parameter curve, an additional condition is required to define the torispherical approximation. This additional condition, which forms the basis for the graphical construction, is that the tangent of the opening angle for the spherical cap portion of the torispherical closure be equal to the ratio of the minor to the major axis for the given ellipse.

8

Thus, the deviation of the numerical value in the column labeled $\frac{1}{\bar{\varphi}_o} \tan^{-1} \frac{\ell}{R_c}$ from unity is a measure of the deviation of the torisphere from a torisphere that approximates an ellipse.

The effect of the boundary conditions, which represent the stiffness of the cylinders to which the closure is attached, on the buckling loads of elliptical and torispherical closures is shown by cases 2 through 4 of table 1 and cases 3 through 5 of table 2. The change in the buckling load is not significant for either closure. This apparently follows from the fact that the circumferential stress resultants near the boundary (at point of attachment to cylinder) are much lower than their maximum values (see figs. 2 and 5) and from the assumption of clamped boundary conditions on the asymmetric buckling mode.

A comparison of buckling loads for torispheres approximating (four-center method) ellipses is shown by cases 1 and 2 of table 1 compared to cases 1 and 2 of table 2. The four-center method produces a better geometrical approximation for ellipses whose ratio of minor to major axis is small than it does for ellipses whose ratio of axes is large. Similarly, the buckling load for the torisphere that approximates the ellipse with a low m/R_c ratio (case 2) is in closer agreement with the ellipse's buckling load than for the ellipse with the larger m/R_c ratio (case 1).

A comparison of the buckling loads for torispherical closures obtained in this study with those reported by Mescall (ref. 2) is shown in fig. 6. As discussed earlier, the main difference between the two sets of results is finite-deflection theory compared to linear theory.

Some of the experimental buckling loads for torispherical closures reported by Adachi and Benicek (ref. 4) are shown in fig. 7 and compared with numerical results from this study. The numerical and experimental buckling loads are in close agreement with each other. For a fixed value of opening angle $\bar{\varphi}_o$ and ratio of toroidal radius to cylinder radius R_t/R_c the data appear to be almost linear on the log-log plot. This was observed by Adachi and Benicek who proposed a relationship of the form

$$\frac{q_{cr}}{E} = C_1 \left(\frac{h}{R_t} \right)^{C_2}$$

9

where C_1 and C_2 are constants that depend on $\bar{\phi}_o$ and R_t/R_c. Figure 8, which shows additional results obtained in this study for torispherical closures, shows that this relationship extends to other values of the parameters $\bar{\phi}_o$ and R_t/R_c.

The numerical buckling loads obtained in this study for elliptical closures with clamped boundary conditions subjected to internal pressure are shown in fig. 9. It was found that ellipses with a ratio of minor to major axis less than $1/\sqrt{2}$ may buckle depending on the ratio of thickness to minor axis. This dependence of stability on thickness and shallowness ratios is shown in fig. 10 and implies that the curves of fig. 9 are bounded on the right. This lack of buckling pressure for some shells is related to the nonlinearity in the increase of compressive stresses with pressure.

CONCLUSIONS

As a shallow dome bulges outward under internal pressure, the maximum stresses fall below the levels predicted by linear theory. This statement applies to midsurface stresses from the circumferential stress resultant N_θ^o and to the stresses from the bending moment M_x^o. The axial stress-resultant N_x^o from finite-deflection theory is nearly the same as predicted by membrane theory.

An effect of this nonlinearity in the axisymmetric stress distribution is that some elliptical closures, although shallower than $\sqrt{2}:1$, do not exhibit any buckling pressure. The possibility of using these shallow domes in aerospace vehicles should be investigated further.

Experiments should be performed to check the assumptions of the analysis. The effect of initial imperfections in shape was neglected in the theory. The good agreement between theory and experiment determined for the torispherical domes indicates that this type of buckling is not imperfection sensitive. The assumption of clamped boundaries requires experiment to define the edge stiffness necessary to produce the stability predicted by the theory.

MARTIN-MARIETTA CORPORATION
    MARTIN COMPANY
        Denver, Colorado, March 15, 1966

APPENDIX

ADDITIONAL TERMS

Functions R_{ij}, H_{ij}, and G_{ij} are defined in reference 5. These functions depend on the coefficients in the homogeneous equations for the asymmetric buckling modes. A nontrivial solution of these equations defines the loads that produce instability.

In changing the computer solution described in reference 5 from a successive approximation solution to a direct solution, some of the R_{ij}, H_{ij}, and G_{ij} functions received additional terms. These terms, listed below, all contain quantities from the axisymmetric prebuckling solution.

Functions from differential equations	Additional terms
G_{11}	$-\alpha_o r_o k_1^2 N_x^o + \alpha_o C k_1 \beta_x^o \left(2\nu \cos \varphi_o - r_o k_1 \beta_x^o\right)$ $- \left(r_o C k_1 \beta_x^o\right)'$
G_{12}	$-n\alpha_o C \beta_x^o \left[\dfrac{(1-\nu)}{2} \sin \varphi_o - \nu r_o k_1\right]$
R_{13}	$-r_o C \beta_x^o / \alpha_o$
H_{13}	$-r_o k_1 N_x^o - r_o k_1 C \left(\beta_x^o\right)^2 + \nu C \beta_x^o \cos \varphi_o + \left(r_o C \beta_x^o / \alpha_o\right)'$
G_{13}	$+\left(r_o k_1 N_x^o\right)' + \left[r_o C k_1 \left(\beta_x^o\right)^2\right]' - \nu\left(C\beta_x^o \cos \varphi_o\right)'$
G_{21}	$-n\alpha_o C \beta_x^o \left[\dfrac{(1-\nu)}{2r_o} \sin \varphi_o - \nu k_1\right]$

Functions from differential equations	Additional terms
G_{22}	$-\alpha_o N_\theta^o \sin^2 \varphi_o - \alpha_o \beta_x^o C (1 - \nu)\left[\cos \varphi_o + \dfrac{\beta_x^o}{2} \sin \varphi_o\right] \sin \varphi_o$ $-\dfrac{r_o(1 - \nu)}{2}\left(C\beta_x^o \sin \varphi_o\right)^{\cdot}$
H_{23}	$\dfrac{nC(1 + \nu)}{2}\beta_x^o$
G_{23}	$\left(n\alpha_o N_\theta^o \sin \varphi_o\right)/r_o + \dfrac{n\alpha_o C(1 - \nu)}{2r_o}\beta_x^o\left(\cos \varphi_o + \beta_x^o \sin \varphi_o\right)$ $-\nu n\left(C\beta_x^o\right)^{\cdot}$
R_{31}	$-\left(r_o C\beta_x^o\right)/\alpha_o$
H_{31}	$r_o k_1 N_x^o + r_o k_1 C\left(\beta_x^o\right)^2 - \nu C\beta_x^o \cos \varphi_o + \left(r_o C\beta_x^o/\alpha_o\right)$
G_{31}	$\alpha_o C\beta_x^o\left[\dfrac{n^2(1 - \nu)}{2r_o} - k_1\left(r_o k_1 + \nu \sin \varphi_o\right)\right]$
H_{32}	$-nr_o C\beta_x^o \dfrac{(1 + \nu)}{2}$
G_{32}	$n\alpha_o N_\theta^o \sin \varphi_o + n\alpha_o C \dfrac{(1 - \nu)}{2}\beta_x^o\left(\cos \varphi_o + \beta_x^o \sin \varphi_o\right)$ $+\dfrac{nr_o(1 - \nu)}{2}\left(C\beta_x^o\right)^{\cdot}$
R_{33}	$\left(r_o N_x^o/\alpha_o\right) + \left(r_o C/\alpha_o\right)\left(\beta_x^o\right)^2$

Functions from
differential
equations

Additional terms

H_{33}

$$-\left(r_o N_x^o / \alpha_o\right)' - \left[\left(r_o C / \alpha_o\right)\left(\beta_x^o\right)^2\right]'$$

G_{33}

$$- n^2 \alpha_o N_\theta^o / r_o - n^2 \alpha_o C \frac{(1 - \nu)}{2r_o}\left(\beta_x^o\right)^2$$

$$+ \left[C\beta_x^o \left(r_o k_1 + \nu \sin \varphi_o\right)\right]'$$

REFERENCES

1. Galletly, G. D.: Torispherical Shells - a Caution to Designers. J. Eng. Ind. (Trans. ASME), vol. 81, series B, 1959, pp. 51-62.
2. Mescall, J.: Stability of Thin Torispherical Shells under Uniform Pressure. (Collected Papers on Instability of Shell Structures.) NASA TN D-1510, Dec. 1962, pp. 671-692.
3. Clark, R. A.: On the Theory of Thin Elastic Toroidal Shells. J. Math. Phys., vol. 29, 1950, pp. 146-178.
4. Adachi, J.; and Benicek, M.: Buckling of Torispherical Shells Under Internal Pressure. Exp. Mech., Aug. 1964, pp. 217-222.
5. Penning, F. A.; and Thurston, G. A.: The Stability of Shallow Spherical Shells Under Concentrated Load. NASA CR-265, July 1965.
6. Thurston, G. A.: Asymmetrical Buckling of Spherical Caps Under Uniform Pressure. AIAA J., Oct. 1964, pp. 1832-1833.
7. Weinitschke, H. J.: On Asymmetric Buckling of Shallow Spherical Shells. J. Math. Phys., June 1965, pp. 141-163.
8. Huang, N. C.: Unsymmetrical Buckling of Shallow Spherical Shells. J. Appl. Mech., Sept. 1964, pp. 447-458.
9. Stein, M.: The Influence of Prebuckling Deformations and Stresses on the Buckling of Perfect Cylinders. NASA TR R-190, Feb. 1964.
10. Almroth, B. O.: Influence of Edge Conditions on the Stability of Axially Compressed Cylindrical Shells. NASA CR-161, Feb. 1965.
11. Thurston, G. A.: Effect of Boundary Conditions on the Buckling of Conical Shells under Hydrostatic Pressure. J. Appl. Mech., Mar. 1965, pp. 208-209.
12. Sanders, J. L., Jr.: Nonlinear Theories for Thin Shells. Quart. Appl. Math., vol. 21, no. 1, Apr. 1963, pp. 21-35.
13. Flugge, W.: Stresses in Shells. Springer-Verlag (Berlin) 1960, ch. 7.
14. Grossman, W. B.: Investigation of Maximum Stresses in Long, Pressurized, Cylindrical Shells. AIAA J., vol. 1, no. 5, May 1963, pp. 1129-1132.
15. Cline, G. B.: Effect of Internal Pressure on the Influence Coefficients of Spherical Shells. J. Appl. Mech., Mar. 1963, pp. 91-97.

TABLE 1

NUMERICAL RESULTS FOR ELLIPTICAL CLOSURES SUBJECTED
TO INTERNAL PRESSURE

$(\nu = 0.3$ all cases)

Case number	$\dfrac{m}{R_c}$	$\dfrac{10^3 h}{m}$	Boundary conditions	$\dfrac{10^6 q_{cr}}{E}$	n
1	0.381	4.05	Cylinder	4.0	80
2	0.251	6.07	↓	1.9	↓
3	↓	↓	Membrane	2.0	65
4	↓	↓	Clamped	↓	↓
5	0.100	5.00		0.10	30
6	↓	10.0		0.19	55
7	↓	15.0		0.61	40
8	0.200	5.00		1.2	50
9	↓	10.0		2.4	55
10	↓	15.0		7.6	45
11	0.300	5.00		2.5	80
12	↓	10.0		13.	55
13	0.400	5.00		7.9	80
14	↓	7.00		18.	50
15	0.100	20.		Stable	
16	0.300	17.5			
17	0.350	15.0			
18	0.450	10.0			
19	0.550	5.0			
20	0.600	2.5	↓	↓	

TABLE 2

NUMERICAL RESULTS FOR TORISPHERICAL CLOSURES SUBJECTED TO INTERNAL PRESSURE

($\nu = 0.3$ all cases)

Case number	$\dfrac{R_t}{R_c}$	$\dfrac{10^3 h}{R_t}$	$\bar{\phi}_o$, deg	$\dfrac{1}{\bar{\phi}_o} \tan^{-1} \dfrac{\ell}{R_c}$	Boundary conditions	$\dfrac{10^6 q_{cr}}{E}$	n
1	0.242	6.39	20.8	1.0	Cylinder	2.6	65
2	0.146	10.4	14.1	↓		1.8	95
3	0.346	4.48	35.0	0.826	↓	6.8	65
4	↓	↓	↓	↓	Membrane	6.7	70
5	↓	↓	↓	↓	Clamped	↓	↓
6	0.146	5.16	14.1	1.0	Cylinder	0.30	130
7	0.167	2.0	35.0	0.662		0.15	200
8	↓	5.0	↓	↓		1.1	125
9	↓	10.0	↓	↓		4.1	100
10	0.194	2.0	27.5	0.775		0.19	120
11	↓	5.0	↓	↓		1.3	90
12	↓	10.0	↓	↓		5.4	70
13	0.242	2.0	20.8	1.0		0.25	100
14	↓	10.0	↓	↓		11.0	65
15	0.346	2.00	19.0	1.27		0.42	85
16	↓	↓	35.0	0.826		1.0	100
17	↓	4.48	19.0	1.27		3.1	55
18	↓	7.00	↓	↓		11.	50
19	↓	↓	35.0	0.826		23.	60
20	↓	9.00	19.0	1.27	↓	23.	50
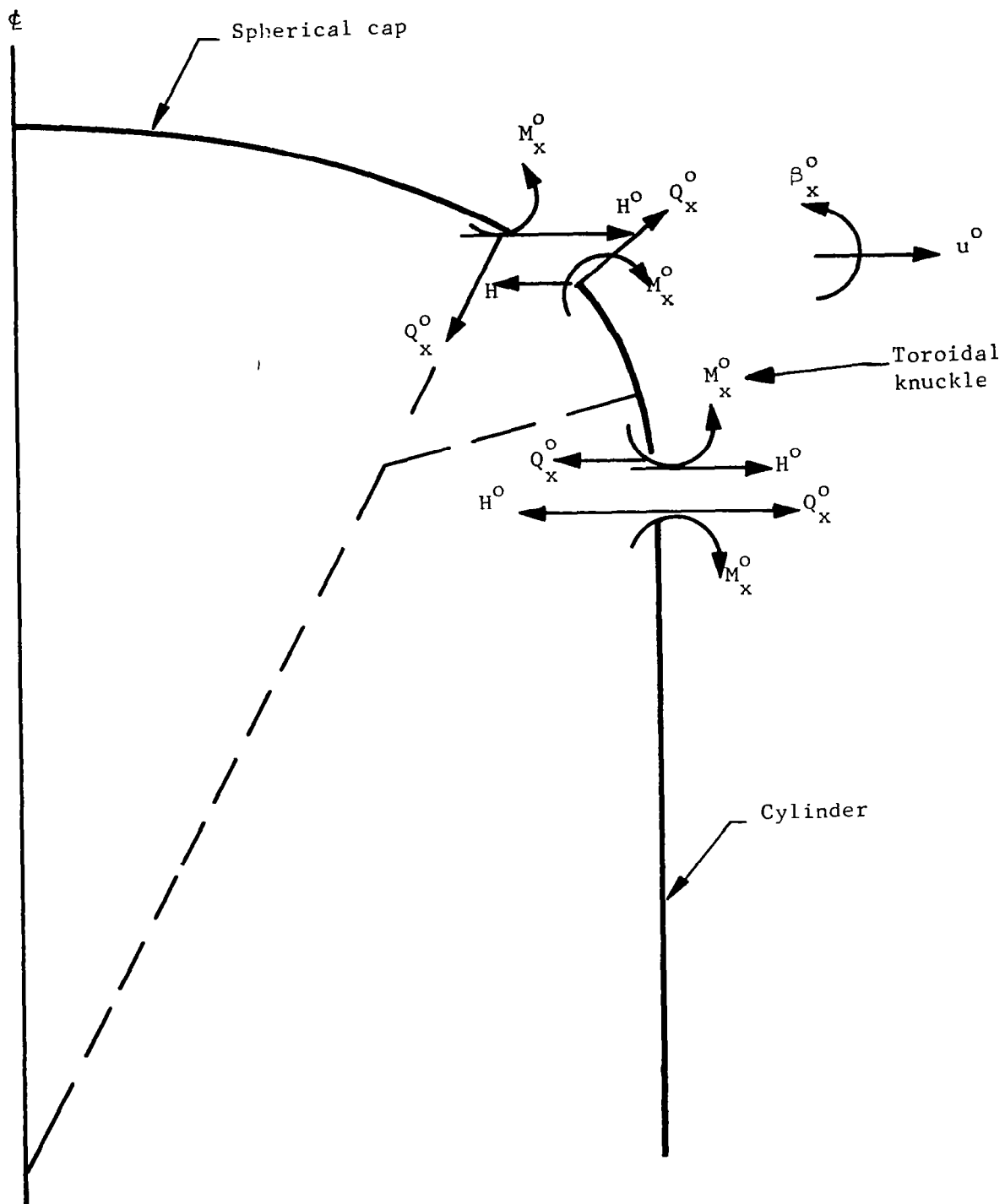
FIGURE 1. -- NOTATION FOR AXISYMMETRIC BOUNDARY CONDITIONS FOR TORISPHERICAL
CLOSURE

N°/hq

Direct stress divided by pressure

Legend:

①   Meridional stress, linear theory
②   Circumferential stress, nonlinear theory, q = 60
③   Circumferential stress, nonlinear theory, q = 80
④   Circumferential stress, linear theory

$\overline{\varphi}_o = 35°$, $\dfrac{R_t}{R_c} = 0.346$, $\dfrac{10^3 h}{R_t} = 4.48$, $\nu = 0.3$

φ, deg
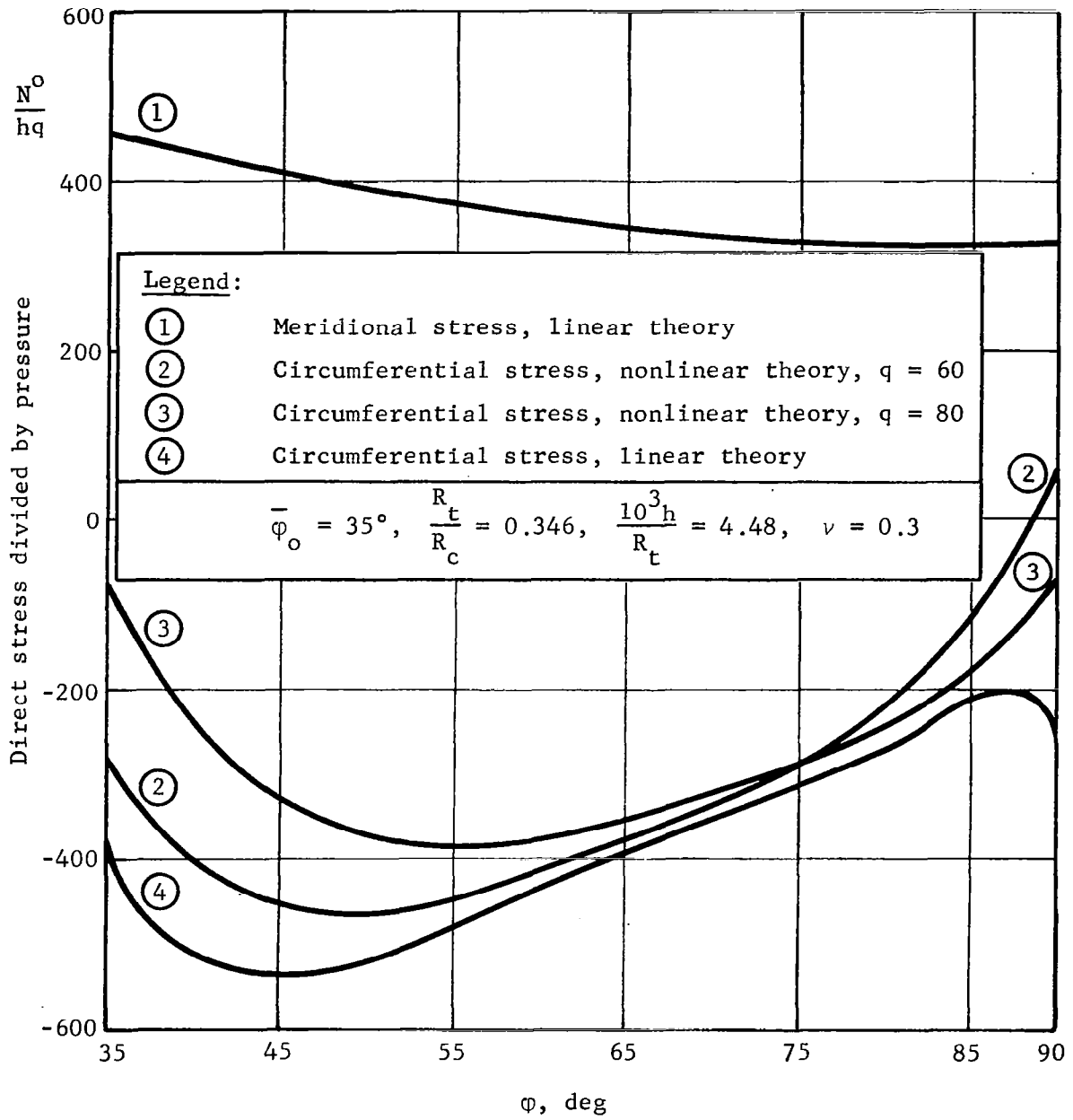
FIGURE 2. -- STRESS DISTRIBUTION FOR TORISPHERICAL CLOSURE
SUBJECTED TO INTERNAL PRESSURE (CYLINDER
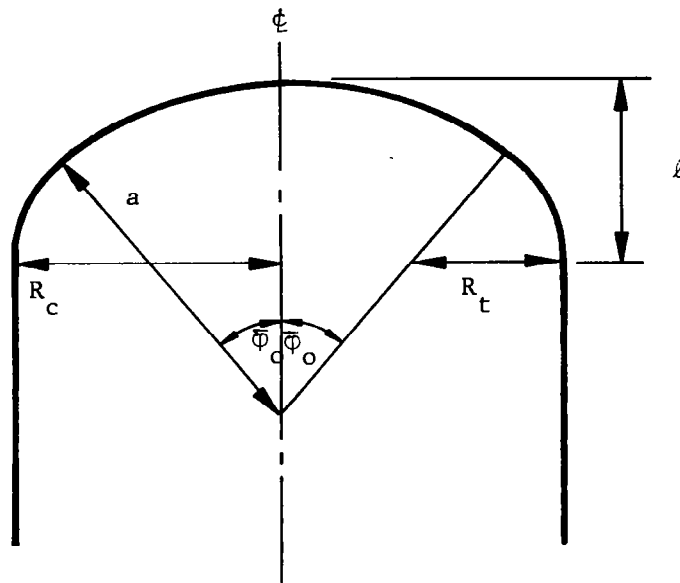BOUNDARY CONDITIONS)

18

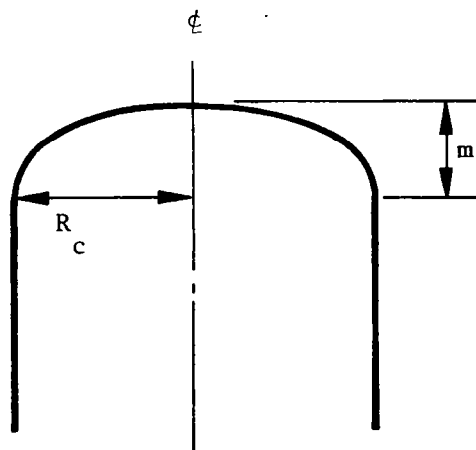FIGURE 3. -- NOTATION FOR TORISPHERICAL CLOSURE

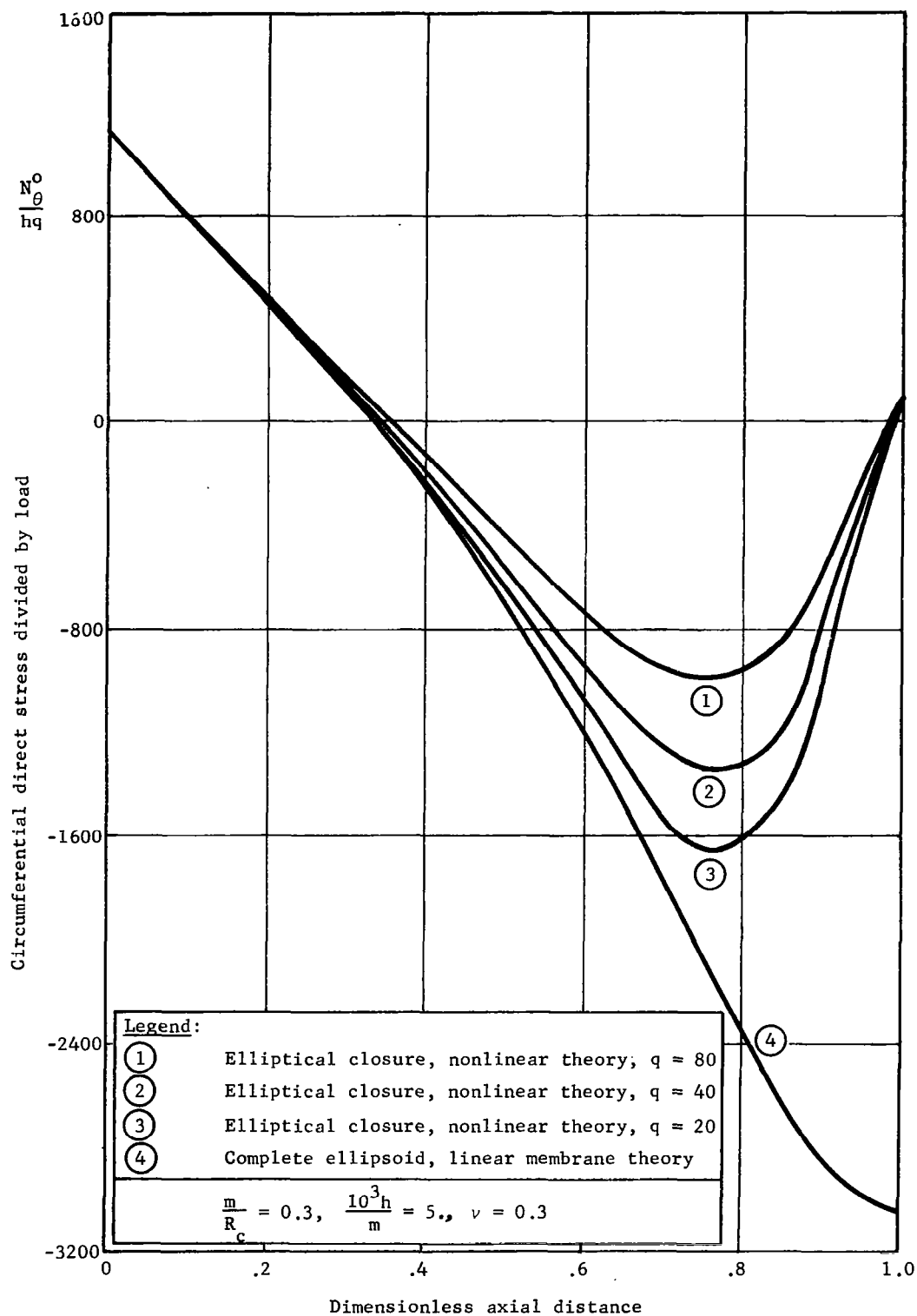FIGURE 4. -- NOTATION FOR ELLIPTICAL
CLOSURE

19

FIGURE 5. -- STRESS DISTRIBUTION FOR TYPICAL ELLIPTICAL CLOSURE SUBJECTED
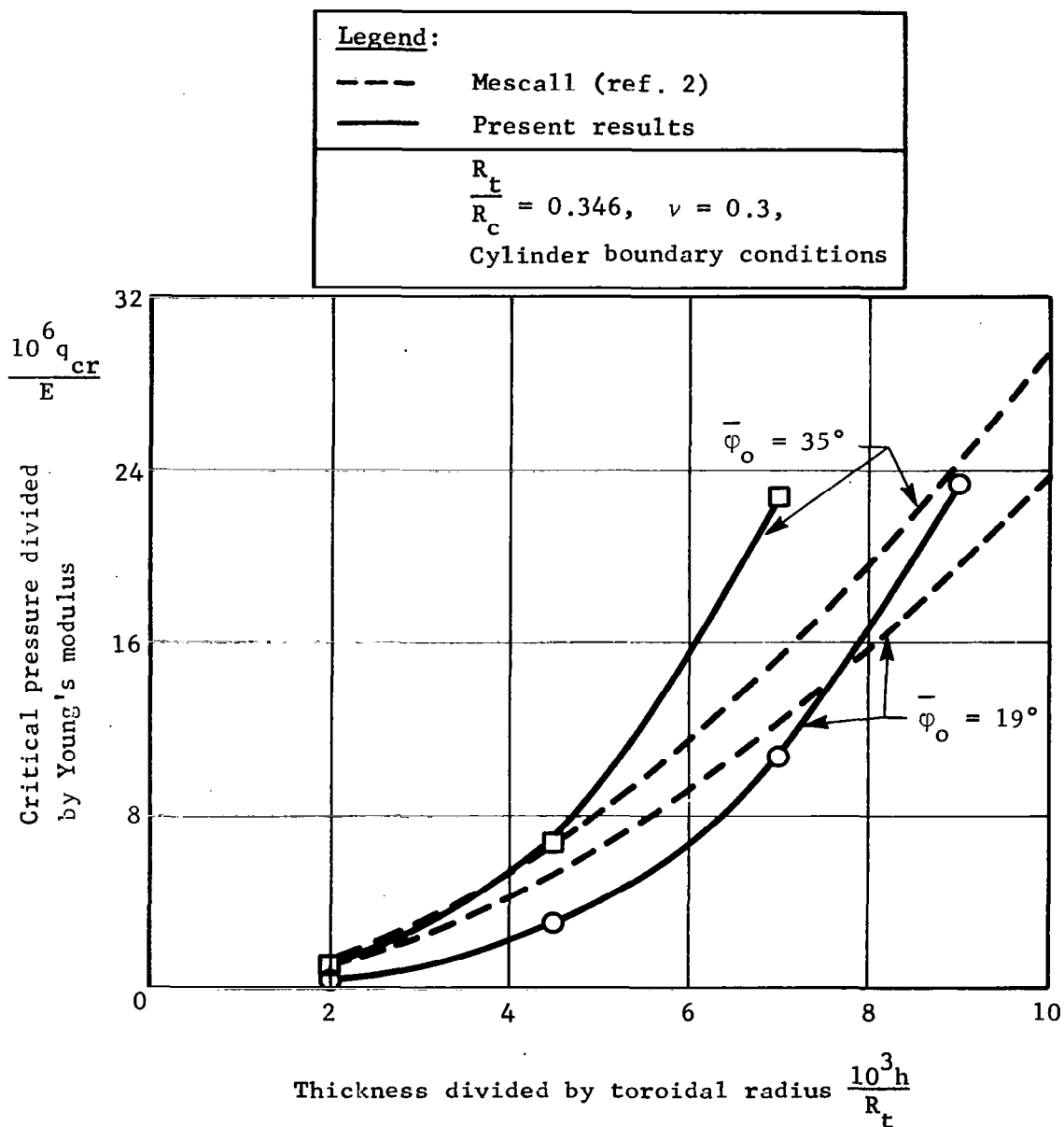TO INTERNAL PRESSURE (CLAMPED BOUNDARY CONDITIONS)

FIGURE 6. -- COMPARISON WITH MESCALL (REF. 2) FOR
TORISPHERICAL CLOSURES SUBJECTED TO
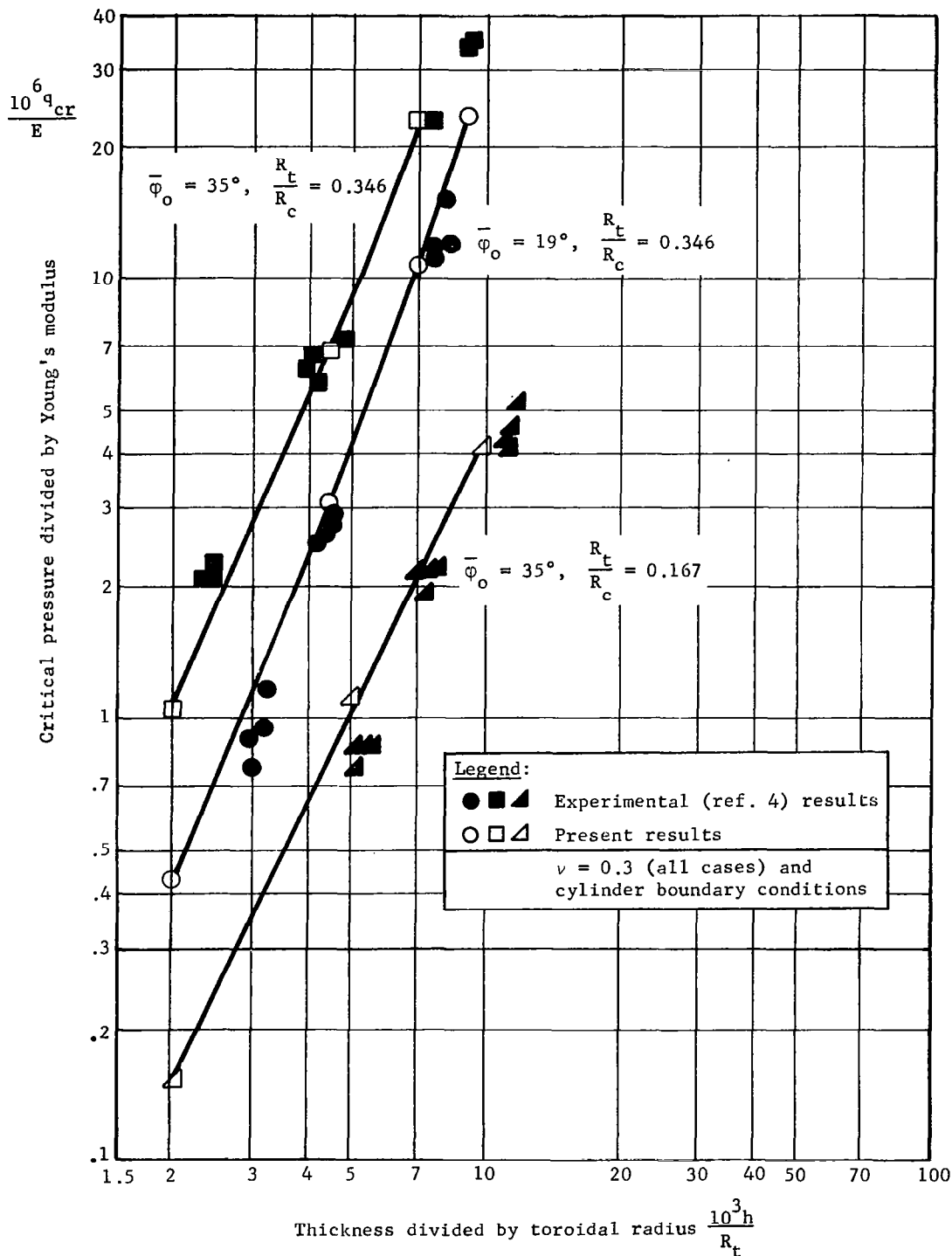INTERNAL PRESSURE

21

FIGURE 7. -- COMPARISON WITH ADACHI AND BENICEK (REF. 4) FOR TORISPHERICAL
CLOSURES SUBJECTED TO INTERNAL PRESSURE

.22

30
20
$\dfrac{10^6 q_{cr}}{E}$
10
7
5
4
3
2
1
.7
.5
.4
.3
.2
.1

Critical pressure divided by Young's modulus

1.5   2   3   4   5   7   10

Thickness divided by toroidal radius $\dfrac{10^3 h}{R_t}$

Legend:

○ $\overline{\varphi}_o = 19°$, $\dfrac{R_t}{R_c} = 0.346$

□ $\overline{\varphi}_o = 35°$, $\dfrac{R_t}{R_c} = 0.346$

◇ $\overline{\varphi}_o = 20.8°$, $\dfrac{R_t}{R_c} = 0.242$

△ $\overline{\varphi}_o = 27.5°$, $\dfrac{R_t}{R_c} = 0.194$

◁ $\overline{\varphi}_o = 35°$, $\dfrac{R_t}{R_c} = 0.167$

◁ $\overline{\varphi}_o = 14.1°$, $\dfrac{R_t}{R_c} = 0.146$

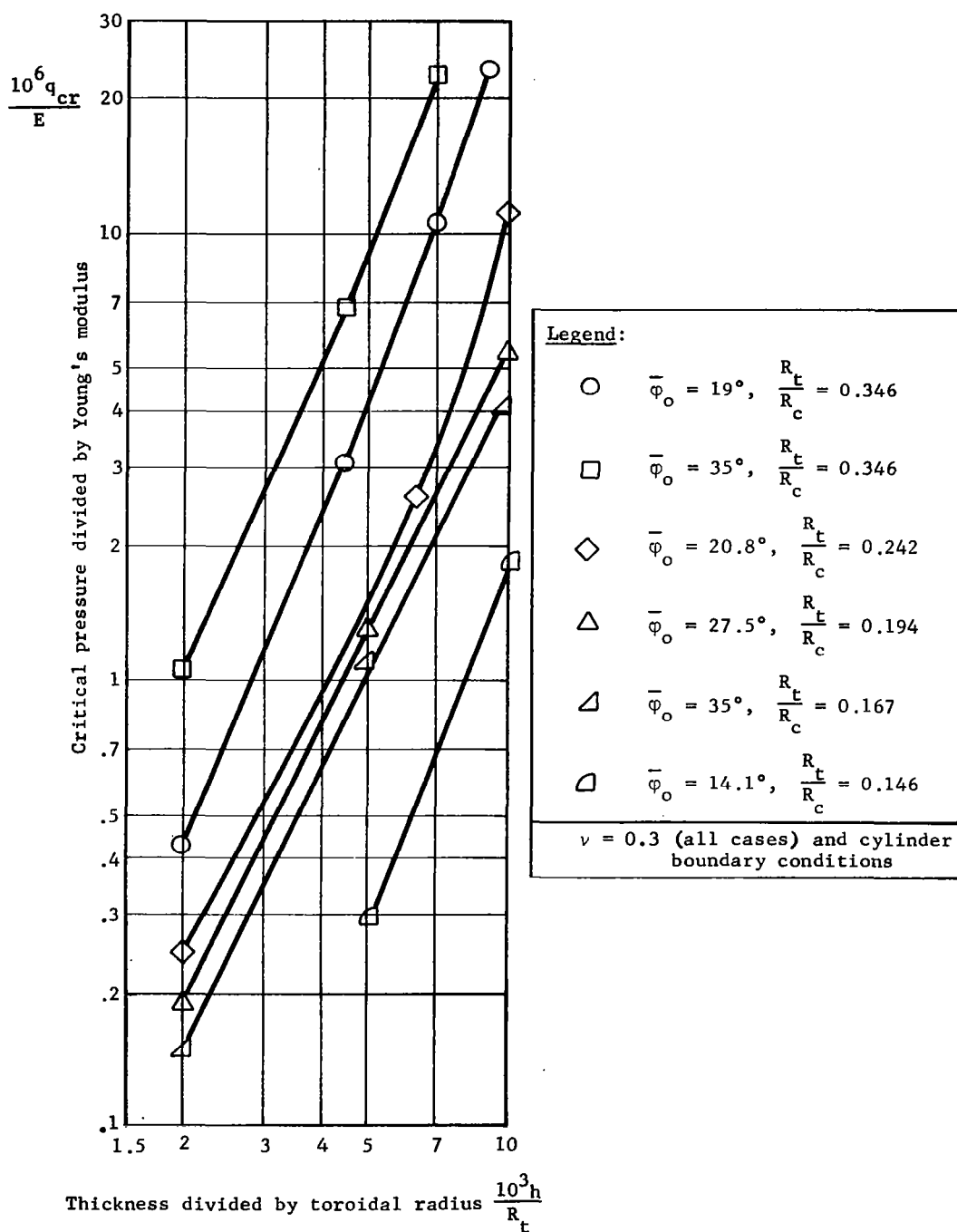$\nu = 0.3$ (all cases) and cylinder boundary conditions

FIGURE 8. -- PRESENT RESULTS FOR TORISPHERICAL CLOSURES SUBJECTED TO INTERNAL PRESSURE
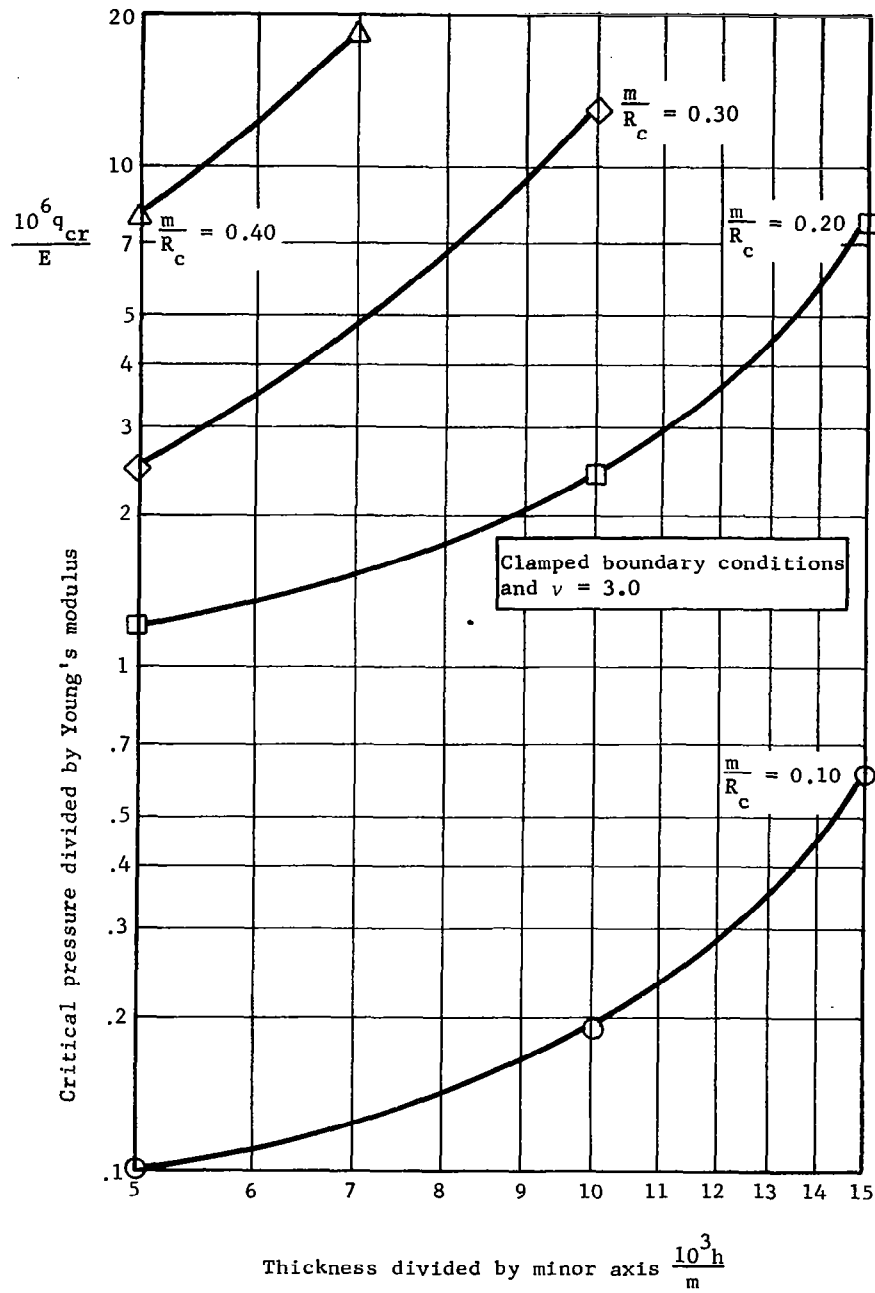
FIGURE 9. -- PRESENT RESULTS FOR ELLIPTICAL CLOSURES SUBJECTED TO
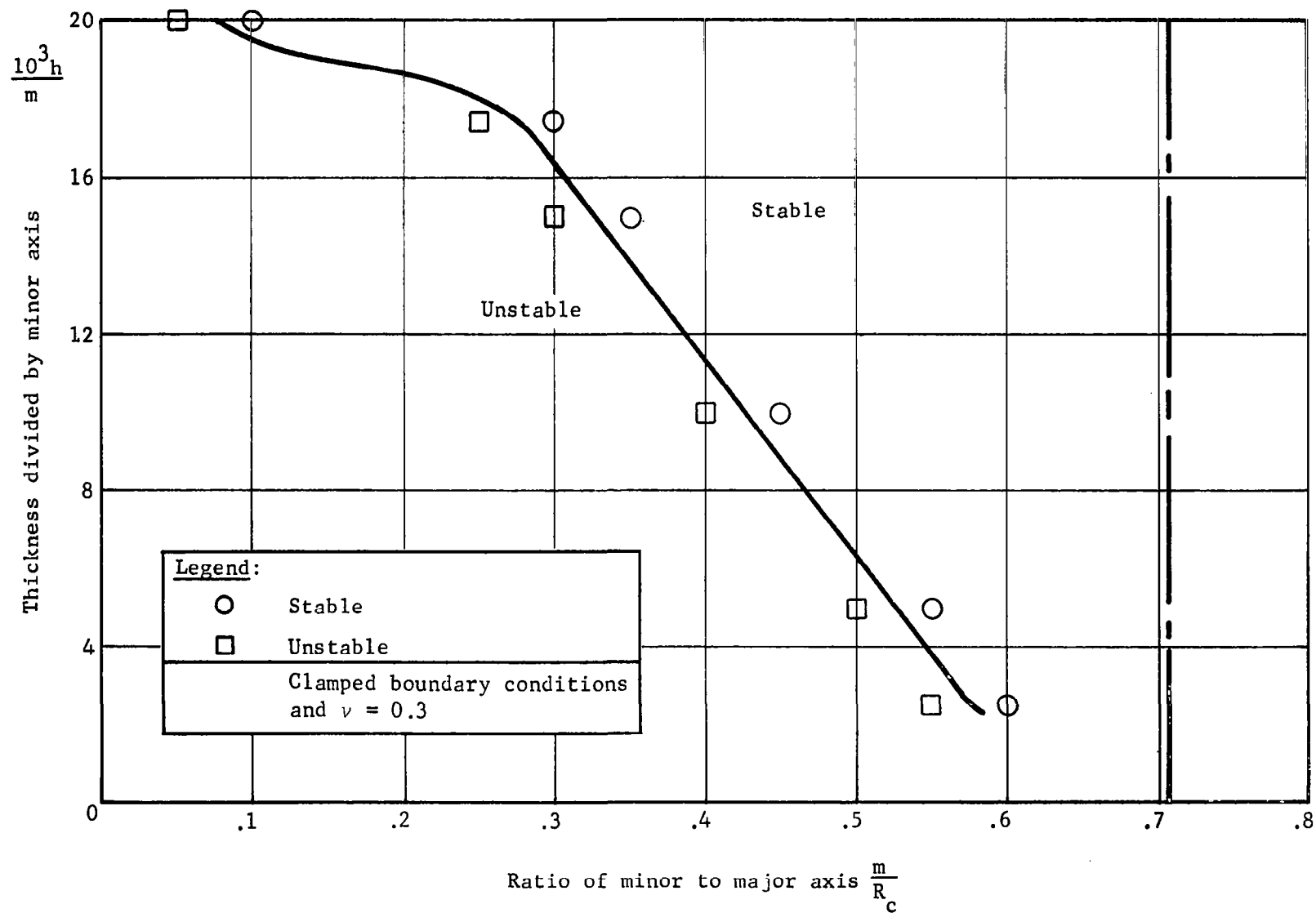INTERNAL PRESSURE

FIGURE 10. -- REGION OF STABILITY FOR ELLIPTICAL CLOSURES SUBJECTED TO INTERNAL PRESSURE

"The aeronautical and space activities of the United States shall be conducted so as to contribute . . . to the expansion of human knowledge of phenomena in the atmosphere and space. The Administration shall provide for the widest practicable and appropriate dissemination of information concerning its activities and the results thereof."

—NATIONAL AERONAUTICS AND SPACE ACT OF 1958

NASA SCIENTIFIC AND TECHNICAL PUBLICATIONS

TECHNICAL REPORTS: Scientific and technical information considered important, complete, and a lasting contribution to existing knowledge.

TECHNICAL NOTES: Information less broad in scope but nevertheless of importance as a contribution to existing knowledge.

TECHNICAL MEMORANDUMS: Information receiving limited distribution because of preliminary data, security classification, or other reasons.

CONTRACTOR REPORTS: Technical information generated in connection with a NASA contract or grant and released under NASA auspices.

TECHNICAL TRANSLATIONS: Information published in a foreign language considered to merit NASA distribution in English.

TECHNICAL REPRINTS: Information derived from NASA activities and initially published in the form of journal articles.

SPECIAL PUBLICATIONS: Information derived from or of value to NASA activities but not necessarily reporting the results of individual NASA-programmed scientific efforts. Publications include conference proceedings, monographs, data compilations, handbooks, sourcebooks, and special bibliographies.

Details on the availability of these publications may be obtained from:

SCIENTIFIC AND TECHNICAL INFORMATION DIVISION

NATIONAL AERONAUTICS AND SPACE ADMINISTRATION

Washington, D.C. 20546